Effect of Solid-State Extrusion on Melting Behavior and Morphology of High-Density Polyethylene

K. Dhawan, D. R. Chaubey, Y.S. Yadav,
P. C. Jain, and V. S. Nanda

*Department of Physics and Astrophysics,
University of Delhi, Delhi-110007, India.*

ABSTRACT: The effect of solid-state extrusion on the melting behavior of high-density polyethylene has been investigated in detail. It was found that ΔT_m, the increase in melting temperature, and ΔH_f, the increase in the heat of fusion, both tend to saturate for values of the extrusion ratio $R > 20$. We have also determined the orientation in the crystalline and the amorphous phases through X-ray and birefringence measurements. It was found that the orientation function f_{am} for the amorphous phase also saturates for $R > 20$. A careful analysis of our results has brought out that, irrespective of the temperature at which the extrudate is prepared, a universal relationship exists between ΔT_m, ΔH_f, and f_{am}. It was further found that when an oriented sample is completely etched, it undergoes fusion at the normal melting temperature of the unoriented polymer. All these findings point to the conclusion that the changes in the melting behavior of high-density polyethylene are brought about essentially by the orientation produced in the amorphous phase.

  KEY WORDS   Polyethylene / Solid-State Extrusion / Melting Characteristics / DSC / Birefringence / X-Rays / Orientation / Crystalline Phase / Amorphous Phase / Etching /

In a semicrystalline polymer, melting is a complex process affected by molecular weight distribution,[1] crystallinity,[2] and the morphology[3] of the sample. Thus, any physical process which brings about structural changes in a polymer inevitably affects its melting characteristics. The effect of drawing on the melting temperature and the heat of fusion of polyethylene has been investigated by Sumita *et al.*,[4] who showed that changes in the melting characteristics are caused mainly by orientation produced in the amorphous phase. Recently, Kojima *et al.*[5] reported similar results in the solid-state extrusion of high-density polyethylene. However, in contrast to Sumita *et al.*,[4] they attribute the increase in melting temperature and heat of fusion to an increase in crystallinity. In order to study the problem in greater detail, we have carried out the solid-state extrusion of high-density polyethylene. Not only the melting characteristics of the extrudates but also the orientation effects in their crystalline and amorphous phases have been investigated through X-ray and birefringence

measurements. It was observed that for a deformation ratio of about 20, the melting temperature, the heat of fusion, and the orientation of amorphous chains along the flow direction tend to saturate. On interpreting the results, we tend to agree with Sumita *et al.*,[4] that the changes in the melting behavior are caused mainly by orientation produced in the amorphous phase.

EXPERIMENTAL

Sample Preparation

The high-density polyethylene used in the present experiment was of commercial grade, GD 6260, supplied by Hoechst Chemicals Ltd., India. The quoted density of the granules of this material is 0.960 g cm^{-3} and the melt index is 0.3 g min^{-1}. On measuring the viscosity-average molecular weight, the value was found to be 1.24×10^5. The actual samples employed in the solid-state extrusion were prepared by recrystallizing the granules in a high-pressure cylinder fitted with a conical die. The

K. Dhawan, D. R. Chaubey, Y. S. Yadav, P. C. Jain, and V. S. Nanda

granules were first brought to the molten state and then cooled to 398 K. To accelerate the process of crystallization, a pressure undercooling of 2 kbar was employed. After an hour, the sample was cooled to the desired extrusion temperature. The density of this sample at the room temperature was found to be $0.9710 \, \mathrm{g \, cm^{-3}}$ which corresponds to the 82 percent weight fraction crystallinity, taking the crystal and amorphous specific volumes[6,7] respectively to be equal to 0.9995 and $1.1755 \, \mathrm{cm^3 \, g^{-1}}$. The details regarding the extrusion procedure are given elsewhere.[8] The effects of various parameters, such as the die angle, capillary bore, capillary length, and extrusion temperature etc. were investigated. The best extrudates were obtained by using a conical die having a 42° cone angle, a 3 to 5 mm capillary bore and an approximately 40 mm length. In every case, the extrudate obtained was in the form of a continuous rod. Due to the conical geometry of the die, the extrusion or deformation ratio increased continuously along the length of the extrudate and acquired a constant value after the material, initially in the conical portion of the die, had been completely extruded. Oriented samples of different extrusion ratios were obtained by cutting thin slices normal to the flow direction at various points from the initial part of the extrudate.

DSC Measurements

A Perkin-Elmer Differential Scanning Calorimeter (DSC-1B) was used with varying sample sizes (3 to 10 mg) and different heating rates (2 to 16 K min^{-1}). The melting temperature T_m and the heat of fusion, H_f were determined, respectively from the location of the peak maximum and the area under the peak of the DSC thermograph. Indium ($T_m = 419$ K and $H_f = 6.8$ cal g^{-1}) was employed as the standard for calibration.

Determination of Crystalline and Amorphous Orientation

Birefringence Δn in samples of various extrusion ratios was measured by means of the retardation method, using a polarizing microscope. The results are shown in Table I. For determining the degree of orientation along the crystal c-axis, wide-angle X-ray diffraction patterns were taken, using a flat plate camera. The orientation function, f_c, was then evaluated by using Herman's type orientation function. For this purpose, azimuthal scannings of

(200) and (020) reflections were carried out and from which $\langle \cos^2 \Phi_{200} \rangle$ and $\langle \cos^2 \Phi_{020} \rangle$ were evaluated by the usual procedure.[9] The degrees of a-, b-, and c-axis orientations, denoted respectively by f_a, f_b, and f_c were then computed from the relations,

$$f_a = \frac{1}{2} (3 \langle \cos^2 \Phi_{200} \rangle - 1) \tag{1}$$

$$f_b = \frac{1}{2} (3 \langle \cos^2 \Phi_{020} \rangle - 1) \tag{2}$$

$$f_c = -(f_a + f_b) \tag{3}$$

The crystalline birefringence Δn_c was determined using the result,

$$\Delta n_c = f_c \Delta n_c^0 \tag{4}$$

where Δn_c^0 is the intrinsic birefringence value of the ideally oriented crystal. Knowing the total birefringence and the birefringence, Δn_c, of the crystalline phase, the firefringence, Δn_a, of the amorphous phase was obtained from the relation,[10]

$$\Delta n_a = (\Delta n - X_v \Delta n_c)/(1 - X_v) \tag{5}$$

where X_v is the degree of volume-fraction crystallinity connected with the weight-fraction crystallinity of the sample by the relation,

$$X_v = \frac{\rho}{\rho_c} X \tag{6}$$

where ρ and ρ_c denote the sample and the crystal phase densities respectively. The values of Δn_c and Δn_a thus obtained are also given in Table I. The amorphous orientation function, f_{am} was determined from the relation,[12]

$$f_{am} = \frac{\Delta n_a}{\Delta n_a^0} \tag{7}$$

In the foregoing calculations, we took $\Delta n_c^0 = 0.0584$ while the value of Δn_a^0 was determined from the relation,[12]

$$\Delta n_a^0 = \frac{\rho_a}{\rho_c} \Delta n_c^0 \tag{8}$$

where ρ_a denotes the density of the amorphous phase. The contribution from the "form birefringence" was neglected.[13]

Nitric Acid Etching

Etching of the oriented samples was carried out

Table I. Variation in the birefringence of the material Δn, birefringence of the crystalline phase Δn_c, and birefringence of the amorphous phase Δn_a with extrusion ratio R (columns (a) and (b) give values for extrudates obtained at 353 K and 388 K, respectively)

R	$\Delta n \times 10^3$		$\Delta n_c \times 10^3$		$\Delta n_a \times 10^3$	
	(a)	(b)	(a)	(b)	(a)	(b)
1	0.0	0.0	0.0	0.0	0.0	0.0
2.5	22.6	22.6	27.5	28.0	3.5	2.3
5	36.8	36.8	43.0	44.3	13.6	8.6
7.5	43.0	43.0	49.5	50.9	18.5	13.3
10	46.8	46.8	52.6	54.4	25.0	17.9
15	48.8	48.8	53.1	54.8	33.5	26.0
20	—	51.3	—	54.8	—	38.0
25	—	52.2	—	54.9	—	41.6
30	—	52.2	—	54.9	—	42.0

with 100 percent fuming nitric acid. Sample chips 2 to 3 mm thick were sealed with an excess of nitric acid in a specially designed glasstube and kept at 335 K for various periods of time. After etching, the samples were washed with distilled water and then by acetone for 8 hours. The samples were then kept at 330 K for about 12 hours to remove all traces of moisture.

RESULTS

In the present study, both the melting temperature T_m and the heat of fusion H_f were found to increase with R, attaining an almost constant value for sufficiently large extrusion ratios. It was found that the effect of the sample size, within the range specified earlier (3 to 10 mg), on T_m and H_f was negligible. However these parameters were found to vary with the heating rate (H.R.). In Figure 1, the variations of T_m with H.R. are shown for two samples ($R=1$ and $R=25$). It may be noted that the extent of superheating in both cases is the same. Thus ΔT_m, which represents the increase in melting temperature due to extrusion with respect to the untreated sample, is independent of the heating rate. A similar result was found to apply in the case of ΔH_f, which represents the increase in heat of fusion due to extrusion. Hence, the extent of orientation brought about by extrusion may best be represented in terms of ΔT_m and ΔH_f.

In Figure 2, the variations in ΔT_m and ΔH_f with R are shown for extrudates obtained at 388 K. It is
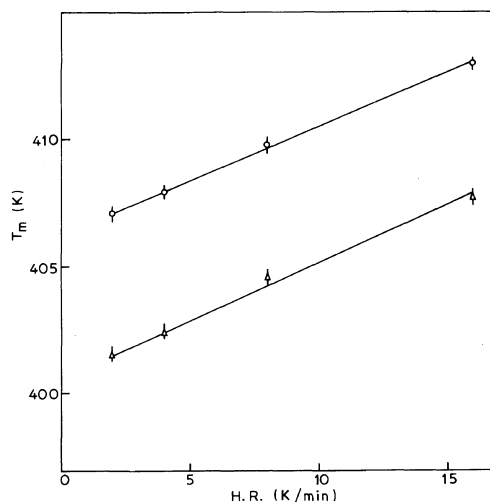
Figure 1. Variation of T_m with heating rate H.R.: lower curve, unextruded material ($R=1$); upper curve, $R=25$.

noted that in both cases the increase is linear for small R, while for $R>20$, the increase is almost negligible. Further, for a given R, T_m was found to depend on extrusion temperature T_{ext}. Such a dependence on $R=15$ is shown in Figure 3. It is seen that with an increase in T_{ext}, T_m increases at first and, after showing a flat maximum, decreases for temperatures close to T_m. A similar trend is observed for the dependence of H_f on T_{ext} and is shown in Figure 4 for $R=15$. From the similarity of

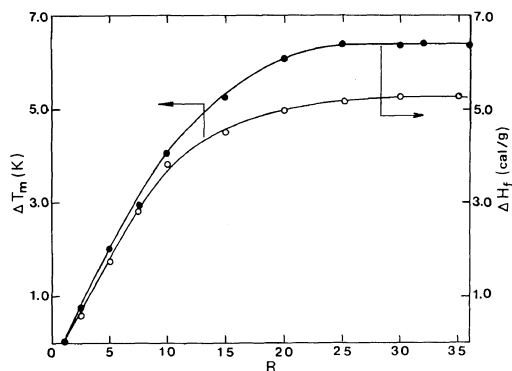K. DHAWAN, D. R. CHAUBEY, Y. S. YADAV, P. C. JAIN, and V. S. NANDA

Figure 2. ΔT_m and ΔH_f as function of extrusion ratio R: $\bigcirc$, ΔT_m values; $\bullet$, ΔH_f values.
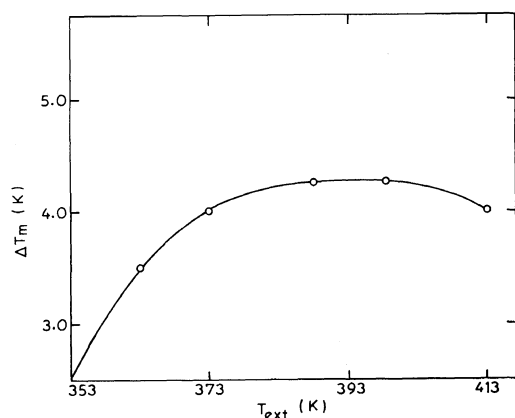

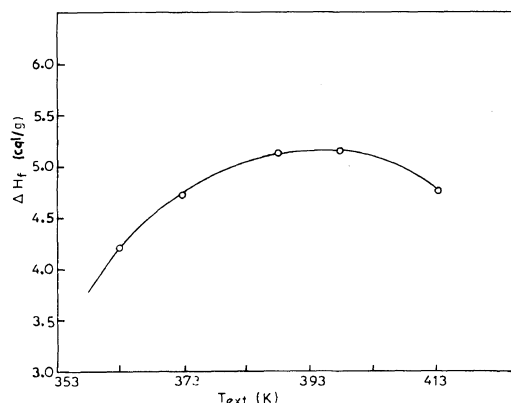**Figure 3.** ΔT_m as a function of extrusion temperature T_{ext} for $R = 15$.

Figure 4. ΔH_f as a function of T_{ext} for $R = 15$.

ΔT_m and ΔH_f plots, it appears natural to suspect a close relationship between these quantities. A plot of ΔH_f as a function of ΔT_m is shown in Figure 5. It may be noted that the experimental points, representing measurements on extrudates prepared at different temperatures (353 to 398 K), lie on a single straight line. The significance of this result is discussed further in the following section.

Kojima *et al.*[5] have also obtained similar results but they have attributed the increase in T_m and H_f solely to the increase in crystallinity on extrusion. In the present study, we measured the density of the extrudate for various values of R and found negligible changes (maximum about 0.1 percent). Since the crystallinity is defined here in terms of density, it may therefore be concluded that the extrusion process does not affect this quantity to any appreciable extent. Consequently the changes in T_m and H_f must be due to some other physical process. This point is considered further in the next section.

The dependence of the amorphous orientation function, f_{am} or R was found to be qualitatively similar to that observed in the case of ΔT_m and ΔH_f. In Figure 6, the variation of f_{am} with R is shown for an extrudate obtained at 388 K. On the other hand,
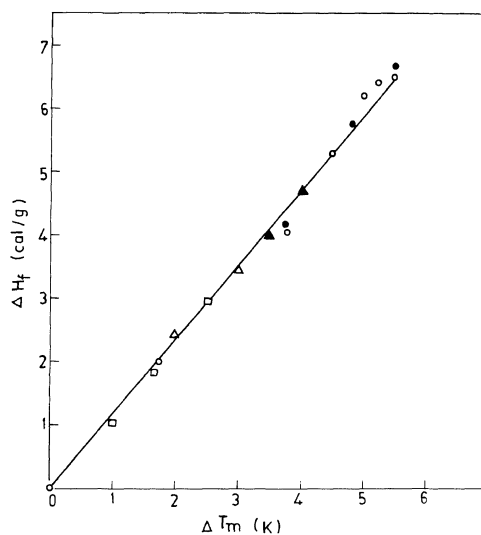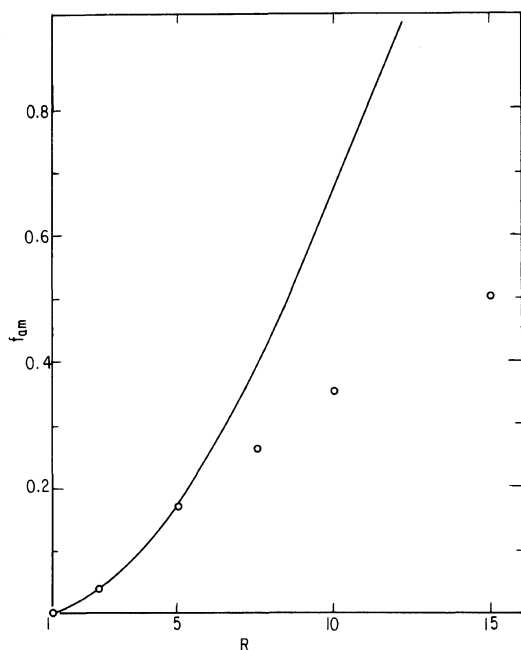

Figure 5. ΔH_f as a function of ΔT_m. Experimental points, $\bullet$, $\bigcirc$, $\triangle$, $\blacktriangle$, and $\blacksquare$, correspond respectively to extrudates prepared at 398, 388, 373, 363, and 353K.

Figure 6. The amorphous orientation function f_{am} as a function of R. The triangles denote the experimental values, the curve represents the variation according to eq 14 of the text. The normalisation of the theoretical and experimental values was carried out for $R = 5$.
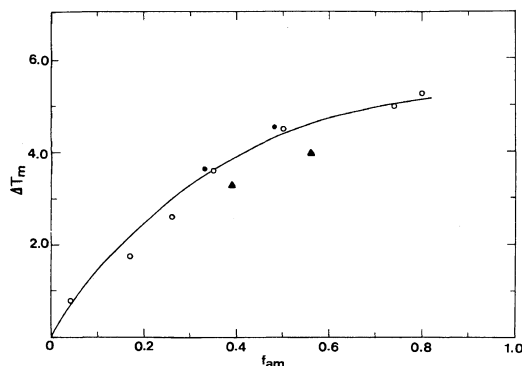
Figure 7. ΔT_m as a function of f_{am}. The rest is as in Figure 5.

Figure 7, which shows the relationship between ΔT_m and f_{am}, serves to underline the relationship between the orientation produced in the amorphous phase and the consequential changes in the melting behavior.

DISCUSSION

The melting of a semicrystalline polymer occurs when the Gibbs free energies G_c and G_a of its crystalline and amorphous phases, respectively, become equal. Following Sumita et al.,[4] we may write for oriented samples (drawn or extruded),

$$G_c = G_{ce} + \Delta G_c \qquad (9)$$

$$G_a = G_{ae} + \Delta G_a \qquad (10)$$

where the suffix, e, denotes the equilibrium value while ΔG gives the change in G brought about by orientation effects. It is easily seen that an increase in G_c lowers T_m, while an increase in G_a raises this value.[4]

The changes in crystal form and morphology contribute to ΔG_c while the orientation of chains in the amorphous phase gives rise to the term ΔG_a. As indicated in the earlier section, the density of polyethylene and hence its degree of crystallinity does not change to any appreciable extent because of extrusion. However, the morphology changes from spherulitic to fibrillar form[14] and a small fraction of the crystalline phase also undergoes a transformation from the orthorhombic to the monoclinic form.[12] The contribution of these transformations to ΔG_c in the melting process, however, may be neglected, as has been explained by Sumita et al.[4] To confirm this, we studied the melting of etched samples. It is expected that after sufficient etching, the chains should be present principally as single traverses of the crystalline regions.[15] We found that the melting temperature of such a sample was the same as that of an unoriented sample. Similar results have been reported by Weeks and Porter.[16] These facts strongly suggest that the changes in T_m and H_f are brought about essentially due to the orientation of chains in the amorphous phase due to extrusion. Sumita et al. have drawn the same conclusion from their investigations carried out with drawn polyethylene. In light of the foregoing conclusions, the observed heat of fusion of an oriented sample may be expressed in the form,

$$H_f = XH_{fc} + (1 - X)H_{fa} \qquad (11)$$

where H_{fc} and H_{fa} stand respectively for the heats of the transformation of the crystal and the oriented amorphous phase to the normal melt. Sumita et al.,[4] on the basis of certain plausible assumptions, have shown that for oriented samples,

K. Dhawan, D. R. Chaubey, Y. S. Yadav, P. C. Jain, and V. S. Nanda

$$\Delta H_{fa} = A\Delta T_m \qquad (12)$$

where A is a constant. Using eq 11 and 12 one finally obtains,

$$\Delta H_f = A'\Delta T_m \qquad (13)$$

where $A' = A(1-X)$. This equation agrees with the observed experimental results shown in Figure 5 and thus supports the contention regarding the role of orientation in the amorphous phase. On the otherhand, the results of this paper clearly negate the point of view advanced by Kojima et al.[5] that the changes in the melting behavior of extruded polyethylene are brought about solely because of the increase in crystallinity. Since, for $R=20$, $\Delta H_f = 6.5$ cal g^{-1} (see Figure 2), it follows according to their hypothesis that X undergoes an increase of about 9 percent. An elementary calculation shows that the density of the extrudate consequently should increase by 1.6 percent, but our measurements, as indicated in the last section, showed only an increase of 0.1 percent.

Next, we turn to the consideration of the amorphous orientation function, f_{am}. According to the theory of rubber elasticity, for an R fold linear extension of a polymer network, we have the expression,[17]

$$f_{am} = \frac{2\pi N(\mu_0+2)^2}{45}\frac{\Delta\alpha}{\mu_0}\frac{1}{\Delta n_a^0}\left(R^2 - \frac{1}{R}\right) \qquad (14)$$

where μ_0 is the refractive index, and N and $\Delta\alpha$ denote respectively the number of network chains per unit volume and the polarizability difference. The curve in Figure 6 represents the variation of f_{am} with R, according to eq 14 where the normalisation of the theoretical and experimental values has been carried out for $R=5$. It is observed that the theory represents the experimental values quite well for low R values. Departures for $R>5$ may be expected and can be attributed to the break down of the theory of rubber elasticity for large deformations.

Finally, we may refer to the significance of the plot of T_m versus f_{am}, shown in Figure 7. The data points representing the results of measurements with extrudates prepared at different temperatures, lie on a single curve just as in the case of ΔT_m versus ΔH_f plot of Figure 5. It may thus be concluded that, for a given polymer ΔT_m and ΔH_f depend only on the value of f_{am}. This further confirms the earlier observation that changes in the melting character of high-density polyethylene are governed essentially by the extent of orientation in the amorphous phase.

REFERENCES

1. P. J. Flory, L. Mandelkern, and H. K. Hall, *J. Am. Chem. Soc.*, **73**, 2532 (1951).
2. R. Chiang and P. J. Flory, *J. Am. Chem. Soc.*, **83**, 2857 (1961).
3. K. Sakurai, T. Oota, K. Miyasaka, and K. Ishikawa, *J. Polym. Sci., Polym. Phys. Ed.*, **14**, 1527 (1976).
4. M. Sumita, K. Miyasaka, and K. Ishikawa, *J. Polym. Sci., Polym. Phys. Ed.*, **15**, 837 (1977).
5. S. Kojima, C. R. Desper, and R. S. Porter, *J. Polym. Sci., Polym. Phys. Ed.*, **16**, 1721 (1978).
6. Y. R. Midha and V. S. Nanda, *Macromolecules*, **10**, 1031 (1977).
7. R. K. Jain, R. N. Gupta, and V. S. Nanda, *J. Macromol. Sci., Phys.*, **B11**, 411 (1975).
8. K. Dhawan, P. C. Jain, and V. S. Nanda, to be published.
9. R. S. Stein, *J. Polym. Sci.*, **31**, 327 (1958).
10. S. Hoshino, J. Powers, D. G. LeGrand, H. Kawai, and R. S. Stein, *J. Polym. Sci.*, **58**, 185 (1962).
11. C. W. Bunn and R. Daubney, *Trans. Faraday Soc.*, **50**, 1173 (1954).
12. K. Nakayama and H. Kanetsuna, *J. Mater. Sci.*, **10**, 1105 (1975).
13. F. A. Bettelhem and R. S. Stein, *J. Polym. Sci.*, **27**, 567 (1958).
14. G. Meinel and A. Peterlin, *J. Polym. Sci.*, A–2, **9**, 67 (1971).
15. A. Keller, *J. Polym. Sci.*, A–2, **9**, 1793 (1971).
16. N. E. Weeks and R. S. Porter, *J. Polym. Sci., Polym. Phys. Ed.*, **13**, 2049 (1975).
17. A. Ciferri, C. A. J. Hoeve, and P. J. Flory, *J. Am. Chem. Soc.*, **83**, 1015 (1961).